

ANDRZEJ WITKOWSKI *, MIROSLAW MAJKUT **

THE IMPACT OF CO₂ COMPRESSION SYSTEMS ON THE COMPRESSOR POWER REQUIRED FOR A PULVERIZED COAL-FIRED POWER PLANT IN POST-COMBUSTION CARBON DIOXIDE SEQUESTRATION

The aim of this paper is to analyze various CO₂ compression processes for post-combustion CO₂ capture applications for 900 MW pulverized coal-fired power plant. Different thermodynamically feasible CO₂ compression systems will be identified and their energy consumption quantified. A detailed thermodynamic analysis examines methods used to minimize the power penalty to the producer through integrated, low-power compression concepts. The goal of the present research is to reduce this penalty through an analysis of different compression concepts, and a possibility of capturing the heat of compression and converting it to useful energy for use elsewhere in the plant.

1. Introduction

Compression of CO₂ is an essential process in the development of carbon capture and storage technologies. A complete CO₂ Capture and Sequestration (CCS) system requires safe, reliable and cost-efficient solutions for transmission of CO₂ from the capturing facility to the location of permanent storage. For transmission of large quantities of CO₂ over moderate distances, pipelines are considered the most cost-efficient solution. Pipeline transmission of CO₂ over longer distances is most efficient when the CO₂ is in the dense phase i.e. in the liquid or supercritical regime (Fig. 1).

This is due to the lower friction drop along the pipeline per unit mass of CO₂ compared to transmitting CO₂ as gas or as a two-phase combination

* Silesian University of Technology, 44-100 Gliwice, ul. Konarskiego 18, e-mail: andrzej.witkowski@polsl.pl

** Silesian University of Technology, 44-100 Gliwice, ul. Konarskiego 18, e-mail: mirosław.majkut@polsl.pl

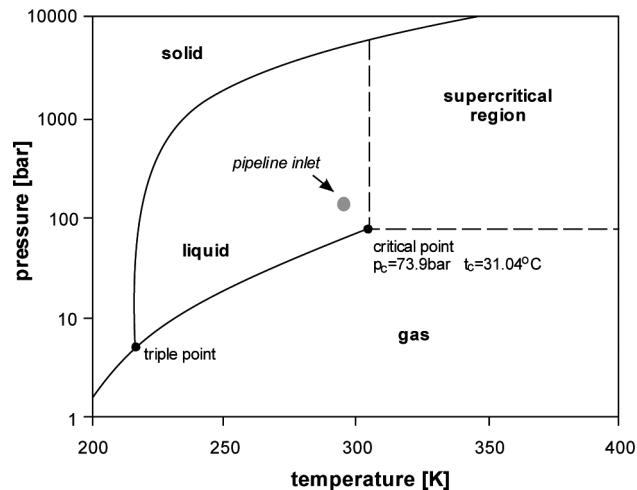


Fig. 1. Phase diagram of CO₂

of both liquid and gas. Pressure losses and sufficient pipeline distances taken into account require compressor discharge pressures in the range of 130-200 bar. Compression of CO₂ differs from most fluid compression tasks due to the high molecular weight, highly compressible behavior and the presence of critical point. At the critical point, the difference between the liquid and the gaseous fluid phase disappears. During the compression process the CO₂ volume reduction is tremendous, resulting in a large impeller diameter at the first – and a very small impeller diameter at the last stage. Existing CO₂ compressors are expensive because the overall pressure ratio is very high (100:1) and, in part, because they require a stainless steel construction to accommodate CO₂ in presence of water vapor. By far the most significant impact on cost is the aerodynamic design practice that limits the design pressure ratio per stage on heavier gases such as CO₂. Thanks to it, CO₂ compressors are responsible for a large portion of the enormous capital and operating cost penalties expected with any carbon capture and sequestration system (CCS). The CO₂ compressor power required for a pulverized coal-fired power plant with amine-based capture systems amounts to approximately 6% to 12% of the plant rating [4], depending on operating conditions, and it cannot be fully optimized without considering the significant amount of heat compression. To optimize heat integration [14], compression systems must be integrated with both power production and CO₂ capture plants. In view of the fact that the selection and design of an efficient CO₂ compression technology is dependent on the applied carbon separation method [13], the present work is motivated by the need to gain a better understanding of the possibilities and limitations of the CO₂ compression process for post-combustion CO₂ capture applications.

2. Boundary conditions and characteristics of the compressing process

The separation technology determines the thermodynamic state of carbon dioxide entering the process. In a typical post-combustion capture process based on chemical absorption, CO₂ is separated from the exhaust gas stream of the power plant at close-to-ambient conditions ($t_1 = 28^{\circ}\text{C}$, $p_1 = 1.5$ bar). The storage of carbon dioxide is accomplished by drilling an injection well into a porous rock stratum or aquifer that is covered by a gas tight cap rock layer. The depth of such geologic formations varies with geographic locations but usually the final pressure of 136-204 bar is required to inject the CO₂ into the formation. For this study, the final pressure of 153 bar was adopted. The compressor power was calculated for the following remaining conditions [15]:

- Power of PC plant 900 MW
- Mass flow of CO₂ 147 kg/s.
- Suction pressure 1.515 bar
- Discharge pressure 153 bar
- Cooling water temperature 15/30°C
- Interstage cooling gas temperature: most optimistic – 20°C and realistic – 38°C
- Pressure loss in the coolers 1-3% ($\Delta p_{max} < 0.344$ bar).

These thermodynamic properties were used throughout the thermodynamic analysis to compare alternative options to the power required for the conventional process.

Additionally, in order to compare the various options and provide accurate values for enthalpy, entropy and density, it was necessary to assume pure carbon dioxide gas for the analysis.

3. Thermodynamic analysis

The process simulation Aspen Plus [3] was used to predict thermodynamic properties of the CO₂ stream at required conditions and quantify the performance of each compression chain option accordingly. Within the Aspen environment, the Benedict, Web, and Rubin with extension by Starling (BWRS) and Redlich and Kwong augmented by Soave (LKP) equation of state for real gases within the relevant ranges of pressure and temperature for process compressor were used. The results for carbon dioxide [13] are as follows: BWRS best agreement for $p_{max} < 50$ bar (>99,8%), LKP best agreement for 50-250 bar (>98%). These findings were compared with the real gas property calculation with the use of the Schultz correction factor [19] and with the gas property tables [2], [5], [7] (Table 1).

Table 1.

Comparison of isentropic four section compressor head calculation options:
 A – Process simulator Aspen Plus [3], AT – Data from thermodynamic tables aided by Aspen Plus [2,7,20], O – calculations of the real gas thermodynamic property with the use of the Schultz correction factor [19], p-i, pressure-enthalpy diagram [1], T – thermodynamic tables [2,7,20]

Section	Y_{sI}	Y_{sII}	Y_{sIII}	Y_{sIV}	$\sum Y_S$
p-i [1]	74.0	68.0	65.0	47.0	257.0
O [13]	75.95	70.44	68.54	48.66	263.58
T [14]	75.51	65.85	66.71	43.85/39.84	251.93
AT [3]	74.33	68.21	66.43	43.11	252.08
A [3]	75.25	72.34	67.30	49.41	264.29

To conform with Table 1, the best consistence between O and A calculation options (>99,7%) was obtained. In the further calculations, Aspen Plus was used to predict the thermodynamic properties of the CO₂ stream at required conditions.

4. Compression technology options

Three variables influence the compressor power consumption and cooling necessities: compressor efficiency, pressure ratio, and CO₂ inlet temperature. The selection and design of a more efficient compression technology is dependent on the carbon dioxide separation method which determines the thermodynamic state of the carbon dioxide entering the process.

The first differentiation between the studied strategies is the density of compressed CO₂, i.e. whether the final compression section constitutes a compressor or a pump. Depending on the compression process, carbon dioxide may remain in vapor form until it reaches the supercritical state or it may be converted into liquid at cryogenic conditions until it reaches the final state as a supercritical fluid. In the latter case, a pump rather than a compressor is used to bring the dense CO₂ to its final pressure. The selected type of the compressor is highly dependent on the starting pressure, which is approximately 1.5 bar. Various types of compressors including ordinary and integrally geared centrifugal machines have been applied to meet these compression service requirements depending on inlet and outlet pressures and volumetric flows. For most CO₂ applications, the integral-gear design offers undeniable advantages [4]. Integrally geared compressors can be optimized for each stage due to lower volume and higher pressure at each progressive stage. It is possible to go to different speeds on each pinion and stage so that very high rpm values (50,000) can be obtained. The polytrophic efficiency of these machines is in high eighties.

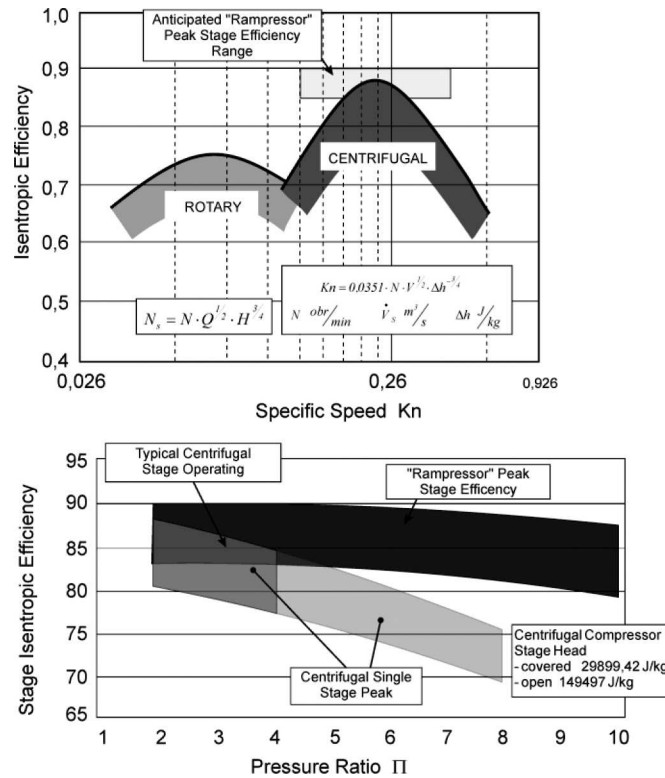


Fig. 2. Competitive advantages and opportunities for shock-wave technology [12]

Aerodynamic challenges include a very high pressure ratio of 1.7 to 2.0:1 and a wide range of flow coefficient stages. At these stage pressure ratios, eight stages of the integral-gear compressor are typically required to reach an overall pressure ratio of 100:1. This issue is further complicated by the need to introduce intercoolers between each compressor stage. The heat of compression discharge temperature associated with these stage pressure ratios is approximately 90°C, which, as the inflow to the next stage, is too high to achieve good efficiency, but it still lacks the thermal driving force for cost-effective heat exchanger selection. This heat is also of insufficient quality to be of practical use elsewhere in the process. The only option is to reject the seventh intercooler heat exchanger. Since CO₂ is a highly corrosive medium, the water content must be reduced to less than 60% of the saturation state. Dehydration of the CO₂ is necessary to avoid corrosion and hydrate precipitation. This requires that H₂O is brought down to ppm-levels. The use of stainless steel for any components in contact with wet CO₂ eliminates the problem.

Lately, a high-efficiency gas compressor [12] has been developed which makes use of the same shock compression technology as is used by su-

personic aircraft inlet systems. This compression is uniquely suited to the compression of large volumes of CO₂ and promises to significantly reduce gas compression auxiliary loads in CCS systems with high efficiency (Fig. 2). In addition to the obvious economic advantages and in view of the fact that the direct result of this compressor makes it possible to achieve single stage compression ratios of 10-12:1, the stage discharge temperature is about 246°C. This offers the potential for significant heat integration, without compromising the compressor performance.

The combination of compression and heat recovery creates an even more impressive energy efficiency advantage by recovering 70-80% of the electrical input energy in the form of useful heat. Potential uses for the available heat are to regenerate amine solutions or pre-heat boiler feed-water.

Either CO₂ is compressed to the desired pressure using a gas compressor or it is liquefied at lower pressures by using refrigeration systems and then pumped to the desired pressure. The final consideration in the analysis was to pump carbon dioxide in a liquid state at a low temperature. The underlying premise of the liquefaction approach is that liquid pumps require significantly less power to raise pressure and are considerably less expensive than gas compressors. The key to minimizing the variable operation and maintenance costs of either CCS system is to integrate the most efficient and variable compression technology with the capture process or the power plant.

5. Overview of CO₂ compression strategies

13 different technically feasible strategies for compressing CO₂ in a coal-fired power plant with post-combustion CO₂ capture according to the boundary conditions specified in Section 2 were studied and will be described below. Their performance was quantified and compared with that of the baseline compressor solution and of the thermodynamic entitlement of isothermal compression. Various types of compressors including a conventional multistage centrifugal compressor, an integrally geared centrifugal compressor, a supersonic shock wave compressor, and pump machines were used.

5.1. Ordinary and integrally geared centrifugal compressors

C1 – The applied baseline thermodynamic analysis to which all others alternatives were compared, the conventional in-line approach which is characterized by four compressor sections with three intercoolers, 14 stage compression and no pump are all schematically illustrated in Figure 3. For this study, the polytropic efficiency of the multistage compressor was taken

at 84% for the first section and linearly reduced in each successive section to 70% for the fourth section. The CO₂ stream is brought to the final pressure value through four compression sections intercooled to 38°C. The analysis so far assumes 29.44°C cooling water, typically from a cooling tower. The process is shown schematically in a pressure-enthalpy diagram in Fig. 4. Option C1 provides a baseline to compare alternative compression options.

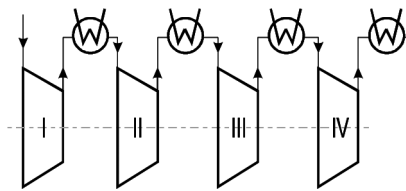


Fig. 3. Basic configuration of four section CO₂ intercooling compression

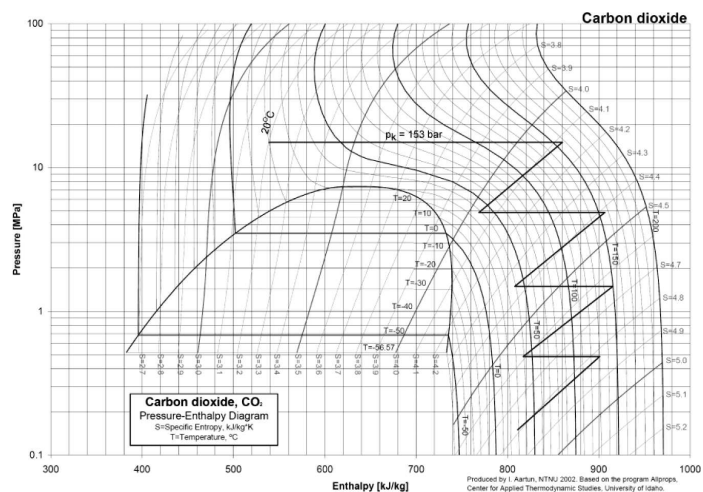


Fig. 4. Thermodynamic path of conventional compression technology. Baseline case C1

C2 – Conventional Centrifugal 16 stage compression with six sections and five inter-cooling steps. The other data are the same as for option C1. A schematic configuration of this compression strategy is shown in Fig. 5. The final cooling step at 38°C is shown in Fig. 6.

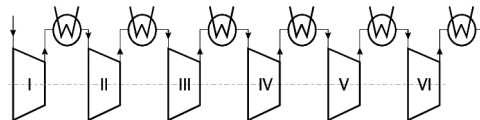


Fig. 5. Configuration of six section intercooling compression

C3 – Eight stage integrally geared compressor with 7 intercoolers (Fig. 7). Polytopic efficiency changes gradually from 84% for the first stage to 70%

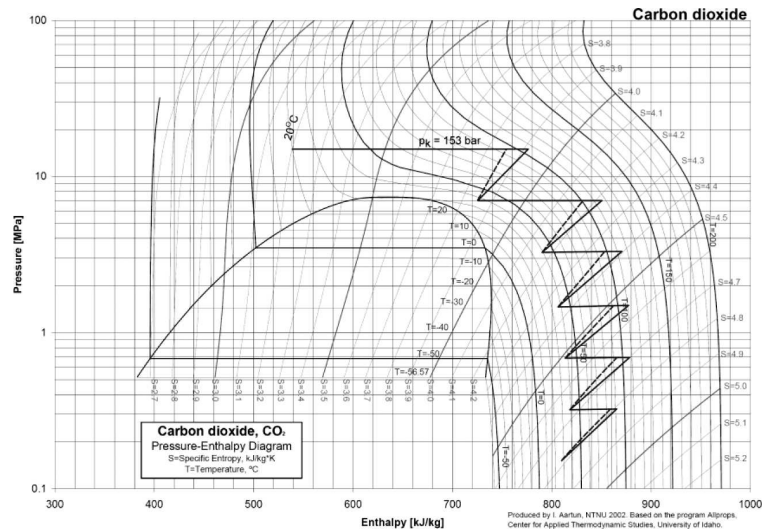


Fig. 6. Thermodynamic path of six section intercooling compression

for the eighth stage. For the comparative analysis of the influence of the inlet gas temperature on the compressor power requirement, the available cooling water at possibly lower ambient conditions (15°C) was firstly used in this option. The adequate inlet gas temperature is 20°C. The thermodynamic path of the compression process is shown in Figure 8.

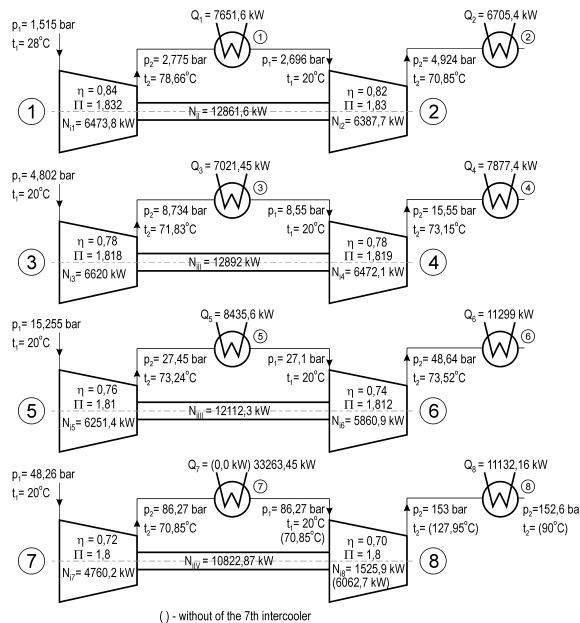


Fig. 7. Schematic illustration of eight-stage integrally geared compressor alternatively with 7 and with 6 intercoolers. Options C3 and C4. Polytropic efficiency $\eta_p = 84\%-70\%$

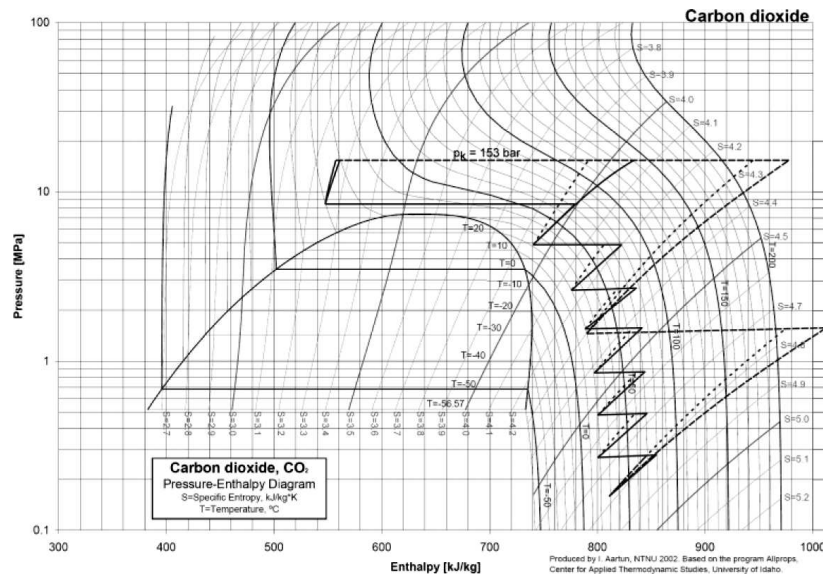


Fig. 8. Comparison of the thermodynamic path of CO₂ compression strategies of eight stage integrally geared compressor with the thermodynamic path of supersonic shock wave two stage compressor. Options C3, C4 and CS1. Interstage compressor cooling 20°C

C4 – Eight stage integrally geared compressor with 6 intercoolers, and inlet inter-stage gas temperature 20°C (Fig. 7). The rejection of the 7th intercooler offers the potential for significant heat integration with the power plant process (Fig. 8). For this study, the adopted efficiency was the same as in concept C3.

C5 – Eight stage integrally geared compressor with 7 intercoolers and inlet inter-stage gas temperature of 20°C (Fig. 9). Polytropic efficiency is 84% for the first stage and 56% for the 8th stage.

C6 – Eight stage integrally geared compressor with 6 intercoolers, and inlet inter-stage gas temperature of 20°C. The rejection of the 7th intercooler offers the potential for significant heat integration with the power plant process. For this study, the adopted efficiency was the same as in concept C5.

C7 – Eight stage integrally geared compressor with 7 intercoolers and inlet inter-stage gas temperature 38°C. The polytropic efficiency is 84% for the first stage and 70% for the 8th stage. The thermodynamic path of the compression process is shown in Fig. 10.

C8 – Eight stage integrally geared compressor with 6 intercoolers and inlet inter-stage gas temperature 38°C. The rejection of the 7th intercooler offers the potential for significant heat integration with the power plant process. For this study, the adopted efficiency was the same as in concept C7.

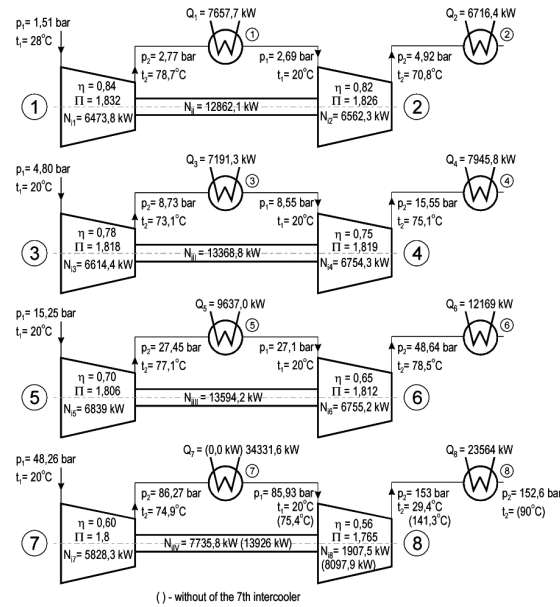


Fig. 9. Schematic illustration of eight-stage integrally geared compressor alternatively with 7 and with 6 interstage coolers. Polytropic efficiency $\eta_p = 84\% - 56\%$. Options C5 and C6

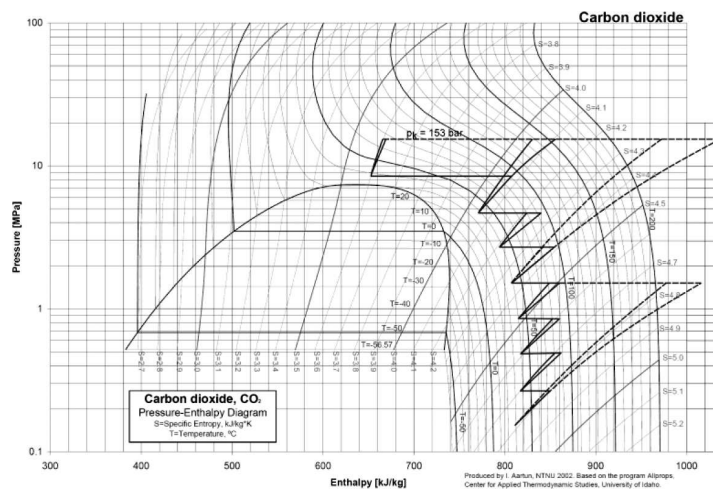


Fig. 10. Comparison of the thermodynamic path of CO₂ compression strategies of the eight-stage integrally geared compressor with the thermodynamic path of Ramgen's supersonic shock wave two stage compressor. Options C7,C8 and CS2. Interstage compressor cooling 38°C

5.2. Advanced supersonic, shockwave compressors

An advanced supersonic two-stage compressor [12] is now being developed for CCS applications. In this work, two options were considered with the following:

CS1 – The compressor concept achieves the required 100:1 pressure ratio in two stages of compression each rated at 10:1 intercooled to 20°C and at increased temperature of 250°C. A schematic illustration of the shock compression is shown in Fig. 11. The thermodynamic path of the compression process is shown in Fig. 8.

CS2 – This option differs from option CS1 with intercooled temperature of 38°C and discharge temperature of 285°C (Fig. 12). The thermodynamic path of the compression process is shown in Fig. 10.

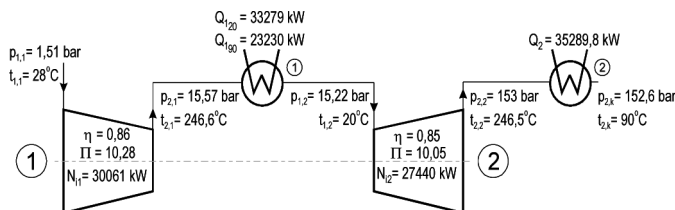


Fig. 11. Schematic illustration of supersonic two stage compressor intercooled to 20°C Option CS1

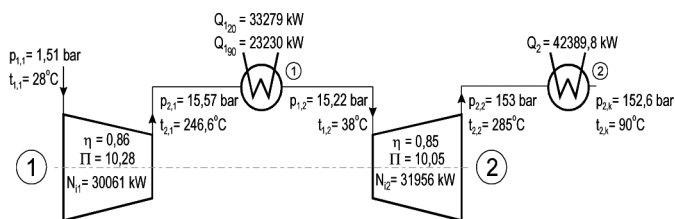


Fig. 12. Schematic illustration of supersonic two stage compressor intercooled to 38°C Option CS2

5.3. Compression and pumping

CP1 – Compression and pumping with supercritical liquefaction. The CO₂ is brought to just above the critical pressure (80 bar) through six compression sections intercooled to 38°C with water at ambient conditions. Subsequent cooling results in the liquefaction of the CO₂ at the compressor outlet pressure of 80 bar, after which a pump is used to bring the dense fluid to the final pressure (Fig. 13). The thermodynamic path of the compression and pumping process is shown in Figure 14.

CP2 – Compression and pumping with subcritical liquefaction. This option uses six compression stages to bring CO₂ to subcritical pressure of 60 bar. This is the minimum pressure required for liquefaction at 20°C with water at ambient condition. After liquefaction under these conditions, the liquid CO₂ is pumped to the final pressure (Fig. 16).

CP3 – Compression and refrigeration pumping (Fig. 15). An absorption refrigeration cycle is introduced in this option in order to evaluate the potential of liquefying CO₂ at a pressure below the minimum of 60 bar evaluated in solution CP2. A low CO₂ liquefaction pressure is desirable in the compression chain in order to maximize the contribution of the less energy-intensive pump to overall pressure. Based on the previous studies [4], [16], a liquefaction pressure of 17.59 bar was selected corresponding to -25°C or -30°C. The combination of ammonia as working fluid and water as solvent is commonly used for this temperature range. The final temperature of CO₂ directly after pumping is very low at -17.16° or -22.46°C (Fig. 16).

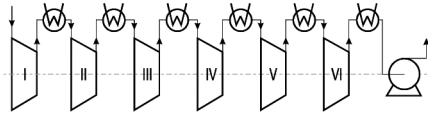


Fig. 13. Schematic illustration of compression and pumping

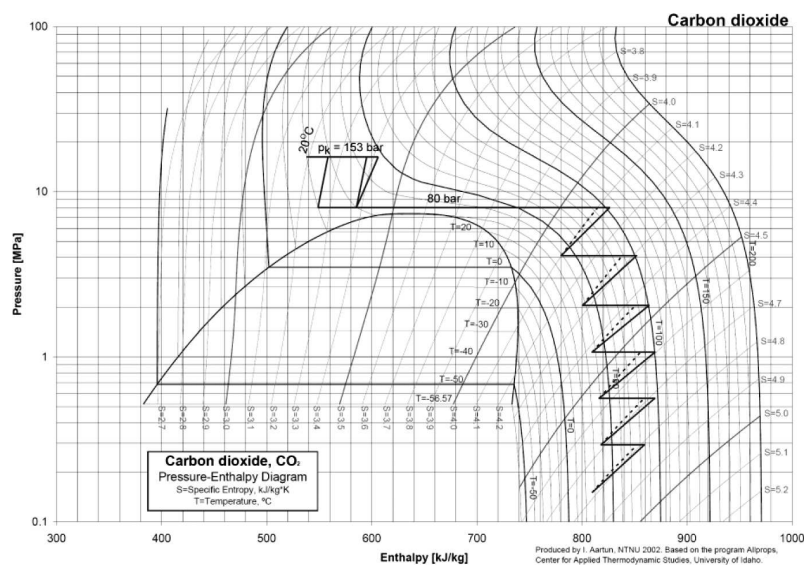


Fig. 14. Thermodynamic path of compression and pumping with supercritical liquefaction

6. Summary of compression options

Table 2 summarizes the compression options considered in the analysis and the power requirement for each thermodynamic process. As the results show, the amount of power required by each compression option varies significantly according to the thermodynamic option. Option C1, the conventional

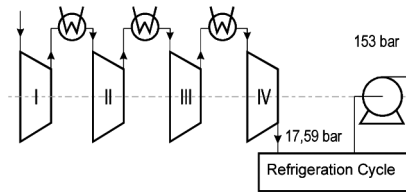


Fig. 15. Schematic illustration of compression and pumping refrigeration cycle

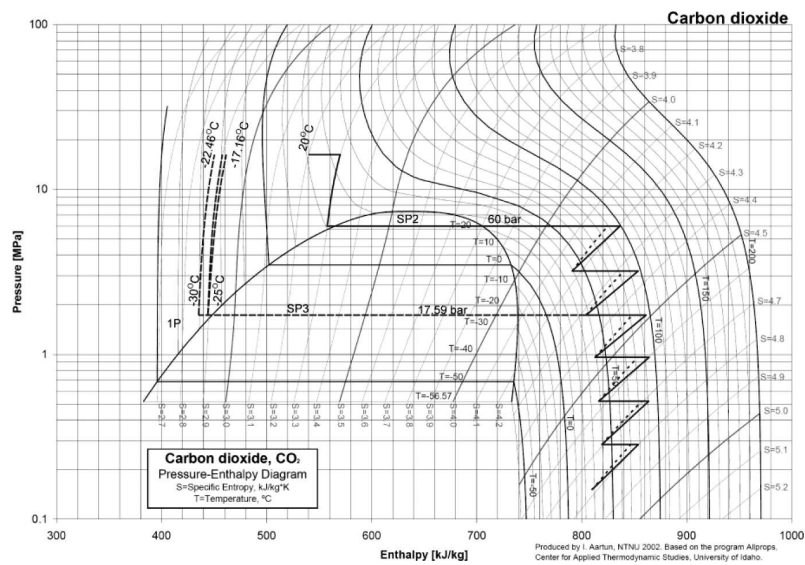


Fig. 16. Thermodynamic path of CO₂ compression and pumping strategies studied. Option CP₂ – compression and pumping with supercritical liquefaction. Option CP₃ – Compression and refrigeration pumping

compression technology, requires total power of 57.787 MW. Option C2 with most intensive cooling provides small compressor power savings above the baseline case (7.5%). Option C3 (Table 2) shows that integrally geared centrifugal compressors with intercoolers between each stage result in significant power savings above baseline case C1. The thermodynamic analysis indicates a 21% reduction in compressor power compared to the conventional process. The latest step of CO₂ compression integration into the power plant is the intercooler heat recovery. Therefore, a certain temperature level must be reached in the heat exchangers to generate useful heat by the rejection of the 7th intercooler in the eighth stage of the integrally geared compressor (options C4, C6 and C8 in Table 2). This disadvantage of having a higher compression temperature after the last stage by leaving the ideal process of isothermal compression can be compensated for by the advantage of heat recovery and power optimization in the plant.

The benefits of the advanced shock wave compression technology when applied to high mole weight gas such as CO₂ are: competitive efficiencies, very high pressure ratio, reduction in weight and reduction in the capital cost when compared with comparable traditional equipment. An additional benefit of the two stage compressor is that the heat of compression discharge temperature is sufficiently high to be useful in the surrounding processes (Table 3). A comparison of energy balance of integrally geared and shock wave compressors are shown in Table 4. The greatest challenge of shock wave compression technology is that significantly higher compression heat can be returned to the overall process in this case.

Table 2.

Comparison of compression technology options

Option	Compression technology	Process definition	Power requirements N_s [kW]	% difference from option C1
C1	Conventional centrifugal 16 stage four section compressor	$P_1 = 1.515$ bar, $P_2 = 153$ bar $t_1 = 28^\circ\text{C}$, interstage suction temp. $t_s = 38^\circ\text{C}$ $\eta_p = 85\div 70\%$	57 787.4	0.0%
C2	Conventional centrifugal 16 stage six section compressor	$P_1 = 1.515$ bar, $P_2 = 153$ bar $t_1 = 28^\circ\text{C}$, $t_s = 38^\circ\text{C}$ polytropic efficiency $\eta_p = 85\div 70\%$	53 443.8	- 7.5%
C3	Eight stage centrifugal geared compressor with 7 intercoolers	$P_1 = 1.515$ bar, $P_2 = 153$ bar $t_1 = 28^\circ\text{C}$, $t_s = 20^\circ\text{C}$ polytropic efficiency $\eta_p = 84\div 70\%$	44 152.5	- 21.2%
C4	Eight stage centrifugal geared compressor with rejection of the 7 th intercooler	$P_1 = 1.515$ bar, $P_2 = 153$ bar $t_1 = 28^\circ\text{C}$, $t_s = 20^\circ\text{C}$ $\eta_p = 84\div 70\%$	48 689.3	- 13.1%
		Heat recoverable to 90°C	11 132.2	- 35.0%
C5	Eight stage centrifugal geared compressor with 7 intercoolers	$P_1 = 1.515$ bar, $P_2 = 153$ bar $t_1 = 28^\circ\text{C}$, $t_s = 20^\circ\text{C}$ $\eta_p = 84\div 56\%$	47 560.5	- 15.2%
C6	Eight stage centrifugal geared compressor with rejection of the 7 th intercooler	$P_1 = 1.515$ bar, $P_2 = 153$ bar $t_1 = 28^\circ\text{C}$, $t_s = 20^\circ\text{C}$ $\eta_p = 84\div 56\%$	53 751.0	- 4,1%
		Heat recoverable to 90°C	14 349.5	- 28,9%
C7	Eight stage centrifugal geared compressor with 7 intercoolers	$P_1 = 1.515$ bar, $P_2 = 153$ bar $t_1 = 28^\circ\text{C}$, $t_s = 38^\circ\text{C}$ $\eta_p = 84\div 70\%$	48 555.1	- 13,4%
C8	Eight stage centrifugal geared compressor with rejection of the 7 th intercooler	$P_1 = 1.515$ bar, $P_2 = 153$ bar $t_1 = 28^\circ\text{C}$, $t_s = 38^\circ\text{C}$ $\eta_p = 84\div 70\%$	52 919.3	5,6%
		Heat recoverable to 90°C	17 664.1	- 36,2%

Table 3.

Options CS1 and CS2

Option	Compression technology	Process definition	Power requirements [kW]	Heat recoverable to 90°C [kW]
CS1	Two stage shock wave compression	$P_1 = 1.528$ bar, $P_2 = 153$ bar $t_1 = 28^\circ\text{C}$, $t_s = 20^\circ\text{C}$ $\eta_p = 86\div 80\%$ $t_{2/2} = 246.5^\circ\text{C}$	57 500.5	58 520.5
CS2	Two stage shock wave compression	as above $t_s = 38^\circ\text{C}$ $\eta_p = 86\div 80\%$ $t_{2/2} = 285.0^\circ\text{C}$	62 016.5	65 619.8

Table 4.

Comparison of energy balance of integrally geared compressors and shock wave compressors

	Integrally geared eight stage compressor $t_s = 20^\circ\text{C}$	Integrally geared eight stage compressor $t_s = 38^\circ\text{C}$	Shock wave compressor $t_s = 20^\circ\text{C}$	Shock wave compressor $t_s = 38^\circ\text{C}$
	Option C4	Option C8	Option CS1	Option CS2
Total inner output $N_{\Sigma i}$ [kW]	48 689.3	52 919.3	57 500.5	62 016.5
Total heat of compression $Q_{\Sigma r}$ [kW]	93 092.2	73 246.4	77 785.0	84 884.6
Total heat recoverable to 90°C $Q_{r90^\circ\text{C}}$ [kW]	11 132.2	17 664.1	58 520.6	65 519.8

Next options use centrifugal compression followed by liquefaction and pumping (options CP1-CP3, Table 5). The results for the cases CP1 and CP2 show that the power requirement can be reduced by up to 14.6% at the compressor outlet pressure of 80 bar and by up to 20.44% at the sub-critical pressure of 60 bar. This minimum liquefaction pressure is dictated by the cooling medium temperature if water at ambient conditions is used. In order to evaluate the potential of liquefying CO₂ at a pressure below the minimum of 60 bar, CO₂ is cooled to a temperature below ambient during liquefaction at cryogenic pressure. As it can be seen in Fig. 16, the stream of CO₂ is brought to liquefaction pressure 17.45 bar through four compression sections intercooled to 38°C with water. Liquefaction is then carried out at -25°C or better at -30°C with the refrigeration cycle, after which CO₂ is pumped to the final pressure. The combination of ammonia as working fluid and water as solvent is commonly used for this temperature range [4]. The final temperature of CO₂ directly after pumping is very low at -22.5°C. The

Table 5.

Summary of compression and pumping power reduction

Option	Compression technology	Process definition	Power requirements [kW]	% difference from option C1
CP1	Six stage integrally geared compressor with five interstage coolers	$P_1 = 1.515 \text{ bar}, P_2 = 80 \text{ bar}$ $t_1 = 28^\circ\text{C}, t_s = 38^\circ\text{C}$ polytropic efficiency: $\eta_p = 0,84 \div 0,72$ $\pi_{st} = 1,937$	$N_c = 46\,750.0$	
	Pumping with supercritical liquefaction	$P_1 = 80 \text{ bar } t_1 = 31^\circ\text{C}$ $\eta_p = 0,8$	$N_p = 2\,582.9$ $N_c + N_p = 49\,332.9$	- 14.6%
CP2	Six stage integrally geared compressor with five interstage coolers	$P_1 = 1.515 \text{ bar}, P_2 = 60 \text{ bar}$ $t_1 = 28^\circ\text{C}, t_s = 38^\circ\text{C}$ polytropic efficiency: $\eta_p = 0,84 \div 0,73$ $\pi_{st} = 1,846$	$N_c = 43\,718.2$	
	Pumping with subcritical liquefaction	$P_1 = 60 \text{ bar } t_1 = 20^\circ\text{C}$ $\eta_p = 0,8$	$N_p = 2\,257.6$ $N_c + N_p = 45\,975.8$	- 20,4%
CP3	Four stage integrally geared compressor with three interstage coolers	$P_1 = 1.515 \text{ bar}, P_2 = 17.59 \text{ bar}$ $t_1 = 28^\circ\text{C}, t_s = 38^\circ\text{C}$ $\eta_p = 0,84 \div 0,756$ $\pi_{st} = 1.846$	$N_c = 28\,910$	
	Refrigerated pumping	$P_1 = 17.59 \text{ bar}, P_2 = 153 \text{ bar}$ $t_1 = -25^\circ\text{C}$ $\rho_2 = 1\,015.89 \text{ kg/m}^3$	$N_p = 2392.7$ $N_T = N_c + N_p$ $N_T = 31\,302.7$	- 45.8%

combination of the integrated gear compression with the liquefaction process resulted in the greatest energy savings at a 45.8% reduction in compression power compared to the conventional process. However, the liquefaction of carbon dioxide requires large amounts of refrigeration energy. A detailed analysis of the refrigeration cycle is not considered in this text.

7. Conclusions

- 13 different feasible strategies for compressing CO₂ in a coal-fired power plant with post-combustion CO₂ capture were studied. Their performance was quantified and compared with that of a conventional compression solution.
- This study emphasizes that total compression power is a strong function of the thermodynamic process and is not only determined by the compressor efficiency.
- The results of this study show that compression power savings of almost 21% compared to the conventional process using integrally geared compressors can be obtained.

- If successful [12], the two stage shock wave technology with a high efficiency and a high pressure ratio compression is expected to reduce the capital cost of CO₂ compression equipment by as much as 50%, and reduce the operating costs of the carbon dioxide capture and sequestration system by at least 15 percent. An additional benefit is that the stage discharge temperature ranges from 246°C to 285°C, depending on the inlet gas and cooling water temperatures.
- The power required for compression could be reduced if CO₂ was first compressed to an intermediate pressure, then cooled and liquefied, and if that liquid was then pumped to the higher pressure level required for pipeline injection.
- The compression power saving of almost 20.4% can be achieved if CO₂ is liquefied during the compression process up to subcritical pressure of 60 bar and then pumped to the final pressure.
- By introducing a refrigeration cycle for the liquefaction process, CO₂ can produce as much as a 45.8% reduction in the compression power compared to the conventional process. However, the compression power reduction is offset by the power loss in the steam turbine as a result of steam extraction required to drive the refrigeration cycle.
- Liquefaction and pumping equipment will entail additional capital expenses, but some of them will be offset by the lower cost of pumps compared to high-pressure compressors.
- Compression heat is a critical source of energy loss which must be integrated into the capture process or the steam cycle of the power plant.

The results presented in this paper were obtained from research work co-financed by the Polish National Centre for Research and Development within the framework of Contract SP/E/1/67484/10 – Strategic Research Programme – Advanced Technologies for Obtaining Energy. Task 1: Development of Technologies for Highly Efficient Zero-Emission Coal-Fired Power Units Integrated with CO₂ Capture.

Manuscript received by Editorial Board, April 17, 2012;
final version, August 19, 2012.

REFERENCES

- [1] Aartun I.: Carbon Dioxide, CO₂, Pressure-Enthalpy Diagram. Based on the Program Alltrops, NTNU 2002. Center for Applied Thermodynamics Studies, University of Idaho.
- [2] Angus S. et al.: International thermodynamic tables of the fluid state – Carbon Dioxide, International Union of Pure and Applied Chemistry (IUPAC), Pergamon Press, 1976.
- [3] Aspen, Version 7.0, User Guide, 2008.
- [4] Boron P.R., Habel R.: CO₂ Compression Challengers. ASME Turbo Expo 2007.

- [5] Botero C., Finkenrath M., Belloni C., Bertolo S., D'Ercole M., Gori E., Tacconelli R.: Thermo-economic Evaluation of CO₂ Compression Strategies for Post-Combustion CO₂ Capture Applications. Proc. of ASME Turbo Expo 2009.
- [6] CO₂ Capture and Storage. VGB Report on the State of the Art. 2004.
- [7] Edmister W.C., and Lee B.I.: Applied Hydrocarbon Thermodynamics. Vol. 1, Second Edition, Gulf Publishing Company, 1984.
- [8] Gresh M.T.: Compressor Performance. Butterworth-Heinemann. Boston, 1991.
- [9] Göttlicher G.: The Energetics of Carbon Dioxide Capture in Power Plants. NETL 2004.
- [10] Kidd H.A., Miller H.F.: Compression Solutions for CO₂ Applications. Traditional Centrifugal and Supersonic Technology. Engineers Notebook. Dresser-Rand.
- [11] Koopman A.A., Bahr D.A.: The Impact of CO₂ Compressor Characteristics and Integration in post Combustion Carbon Sequestration Comparative Economic Analysis. Proc. of ASME Turbo Expo 2010.
- [12] Lawlor S.: CO₂ Compression Using Supersonic Shock Wave Technology. Ramgen Power System, September 15, 2010.
- [13] Lüdtker K.H.: Process Centrifugal Compressors. Springer Verlag Berlin Heidelberg 2004.
- [14] Łukowicz H., Chmielniak T., Kochaniewicz A., Mroncz M.: An Analysis of the use of Waste Heat from Exhaust Gases of a Brown-Coal Fired Power Plant for Drying Coal. Rynek Energii nr 1, February 2011.
- [15] Łukowicz H., Mroncz M.: Basic Technological Concepts of a "Capture Ready" Power Plant, Energy & Fuels, DOI: 10.1021/ef201669g.
- [16] Moore J.J., Nored M.G.: Novel Concepts for the Compression of Large Volumes of Carbon Dioxide. Proceedings of ASME Turbo Expo 2008.
- [17] Moran M.J., Shapiro H.N.: Fundamentals of Engineering Thermodynamics. John Wiley & Sons, Inc. New York, 1988.
- [18] Ramgen Power Systems: Workshop on Future Large CO₂ Compression Systems. Gaithersburg, March 30-31, 2009.
- [19] Schultz J.: The polytropic Analysis of Centrifugal Compressors. Journal of Engineering for Power, January 1962.
- [20] Span R. and Wagner W.: A New Equation of State for Carbon Dioxide covering the Fluid Region from the Triple Point Temperature to 1100 K at a Pressure up to 800 MPa. J. Phys. Chem. Ref. Data. Vol. 6, pp. 1509-1596, (1996).
- [21] Szargut J.: Termodynamika techniczna. Wydawnictwo Politechniki Śląskiej, Gliwice, 2000.
- [22] VDI 2045: Acceptance and Performance Tests on Turbocompressors and Displacement Compressors. Theory and Examples. Düsseldorf 1993.

Wpływ procesu sprężania na moc sprężarek do dwutlenku węgla wychwyconego ze spalin bloku energetycznego na pył węglowy

Streszczenie

Celem niniejszej pracy jest analiza różnych procesów sprężania CO₂ wychwyconego ze spalin bloku energetycznego o mocy 900 MW na pył węglowy. Przedstawiono szereg różnych procesów sprężania i określono zużycie energii każdego z nich. Szczegółowa analiza termodynamiczna umożliwiła określenie sposobów zminimalizowania kosztów energii poprzez dobór najskuteczniejszego procesu sprężania oraz wykorzystanie ciepła sprężania w obiegu ciepłym siłowni.